IECO International Journal Of Industrial Electronics Control and Optimization
Print ISSN: 3517-2645
Online ISSN: 3568-2645
Homepage: https://ieco.usb.ac.ir/

An Ultrasonic Transmission/Reflection Mode Tomography for Two-Phase Flow Measurement

Omid Qorbani[1] and Esmaeil Najafiaghdam[2]

Faculty of Electrical Engineering, Sahand University of Technology, Sahand Town, Tabriz, Iran[1,2]
Corresponding author's email: najafiaghdam@sut.ac.ir

Article Info

Article type:
Research Article

Article History:
Received 2022-05-16
Received in revised form 2022-07-06
Accepted 2022-07-14
Published online 2022-08-31

Keywords:
Multiphase Flow,
Reflection-Mode,
Tomography,
Ultrasonic Process.

ABSTRACT

The ultrasonic process tomography obtains the distribution of two-phase flows based on ultrasound propagation in different fluids, so it is valuable for industrial monitoring and measurement. It can do a non-intrusive exploration of the multi-phase flow hydrodynamics. This paper presents a dual-mode ultrasonic process tomography that fuses reflection-mode tomography and time-of-flight ultrasonic tomography. In this method, a 32-digit array of ultrasonic sensors is used for flow measurement. The two-phase flow rate that involves liquid and gas phases is calculated by a simple algebraic algorithm with the data obtained from sensors. Simulation results reveal that the measurement technique is independent of the fluid flow pattern and the system error is also decreased. The contribution of the article is the introduction of a simple algebraic method for image reconstruction for which no special case is considered and simultaneously, the image reconstruction error is reduced. The relative error of the reconstructed images is presented by MATLAB simulation and it is much lower than the conventional methods. For a gas bubble with ultrasonic wave reflection time from its surface, the simulation results show that the spatial imaging error (SIE) factor is less than 2%.

I. Introduction

Nowadays, measuring single-phase and multi-phase fluid flow is a major challenge in the industry. Flowmeters are used for production process monitoring, production management, and the control and optimization of processes [1]. So, it plays a vital role in the continuous measurement and better monitoring of industrial processes [2-8]. Multi-phase flow measurement is used in petroleum exploration, chemical and food industries, nuclear reactors, cardboard industry, and medical applications [9].

Multiphase flow-metering is performed in invasive and noninvasive modes [10, 11]. As long as tools are placed inside the tube, measurement mode is called invasive and fluid has friction with the sensors. In this case, pattern variation of fluid flow reduces the system accuracy. The lifetime of such tools is shorter than noninvasive ones. X-ray, gamma-ray, radioactive sensors, ultrasonic waves, and magnetic waves are categorized as noninvasive measurement sensors [12]. Ultrasonic waves are used for medical imaging, fluid flow measurement, and non-destructive testing. Slow propagation velocity and temperature dependence are the constraints of ultrasound waves [5, 10, 13-15]. Moreover, in analogy with the noninvasive sensors, ultrasonic waves have some benefits. They consume less energy and are less costly. Also, their scale-up are performed easily [16].

We can create a cross-sectional image from tube fluid flow with tomography, and this is tomography's advantage in the industry [5]. Industrial process tomography is a harmless and noninvasive imaging technique that uses many physical sources. In addition to radiation sensors like X-rays and gamma rays, ultrasound can also be used for tomography. Ultrasound waves are used for both transient-mode tomography (UTT) and reflection-mode tomography (URT). Optical coherence tomography (OCT), electrical methods such

DOI : 10.22111/IECO.2022.42396.1430

as ECT, EIT, and ERT, and multi-model tomography are other industrial tomography techniques [4, 6, 9, 10, 15, 17].

Ultrasonic tomography outperforms radiation bases tomography methods, and its small wavelength shows an excellent spatial resolution. When it comes to the measurement of a two-phase fluid flow containing gas and liquid, ultrasonic tomography is very suitable [18, 19]. Nondestructive, noninvasive, no moving parts, and online operation are advantages of ultrasonic tomography. Ultrasonic tomography also is less expensive than other techniques. It has widespread usage in biotechnology, medical industries, and reactors. It can be said that one of the most common applications of ultrasound is its diagnostic authenticity in medicine [8, 14, 20, 21]. As mentioned, the key benefits of ultrasound tomography are that it is nondestructive, noninvasive, and inexpensive and that it is operated online [10]. This technique is composed of UTT and URT. We can use both ultrasonic tomography techniques in solitude, but combining UTT and URT gives us many advantages that are better than the single modality of UTT or URT [22].

There are various techniques for image reconstruction, and algorithm selection depends on the tomography techniques. Back projection algorithm, filtered back projection algorithm (FBP), and algebraic reconstruction techniques (ART) are well known in the literature [5, 6, 23].

II. Principles and Construction

Piezo-electric converts mechanical quantity into electrical quantity, or vice versa and a transducer is a device that works in both directions [24, 25].

$$N_{near} = \frac{(2R_T)^2 - \lambda_{aco}}{4\lambda_{aco}} \approx \frac{{R_T}^2}{\lambda_{aco}} \tag{1}$$

Equ. (1) is calculated from the sound intensity, where R_T and λ_{aco} are the piezoelectric diameter and wavelength of the sound, respectively. Aperture size for sound propagation equals the piezoelectric diameter. The first zone is called the near field or Fresnel zone (Fig. 1). Beyond the near field, the pressure of the sound decreases monotonically and this region is called the Fraunhofer zone. Theta is the half-angle of the main lobe divergence for the wave propagation in the Fraunhofer zone. It is characterized by the wavelength and diameter of the piezo-electric and is shown by Equ. (2) as follows [24]:

$$\theta = arc\ sin\,(\frac{1.22\lambda_{aco}}{d}) \tag{2}$$

In ultrasound tomography, the above propagation area and radiation angle of the ultrasound wave (θ) must be considered.

$$R_p = \frac{Z_2 - Z_1}{Z_2 + Z_1}\ . \tag{3}$$

$$T_p = \frac{2Z_2}{Z_2 + Z_1}\ . \tag{4}$$

in which R_p, T_p, Z_1 and Z_2 represent ultrasound pressure reflection, transmission coefficients, and the acoustic impedance of the media, respectively.

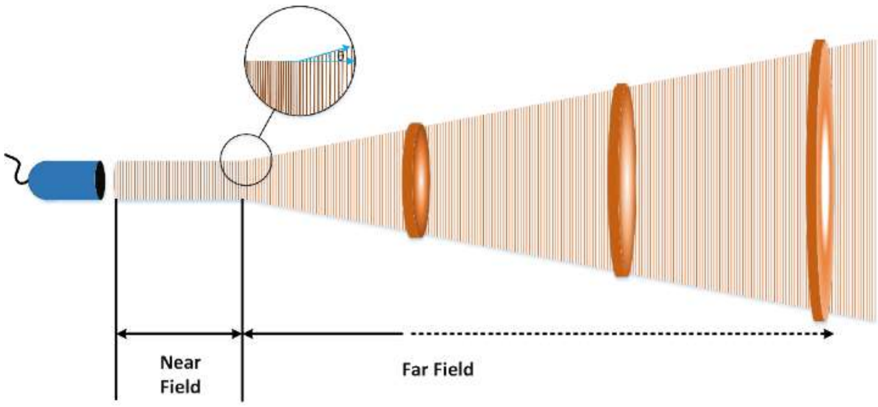

Fig. 1: Near field and far field for piezoelectric

According to Equ. (3) and Equ. (4), the pressure reflection from the gas (air) and liquid (water) interface is about 99.94%. The wave returned from the gas/liquid interface is a significant amount because the value of the reflection coefficient for this interface is large. Then, we can utilize it to determine the location of the bubbles inside the pipe. On the other hand, the wave amplitude attenuation inside the media is essential. When ultrasound waves propagate through the media, the amplitude attenuation of the waves can be depicted as follows:

$$p_z = p_0 e^{-\alpha z} = p_0 e^{-\alpha_0 f_c z} \qquad (5)$$

where p_0 is the sound pressure at the distance of z=0, p_z is the sound pressure at z, α_0 is the attenuation coefficient of media, and f_c is the piezo-electric frequency [22, 26].

III. Proposed Method

To simulate the proposed method, the diameter of the pipe is assumed 130mm and the frequency of the piezoelectric is assumed 1 MHz because choosing the central frequency of the piezo-electric determines the measurement accuracy [25]. By calculating the quantities from Equ. (1) and Equ. (2), it can be determined that the five sensors in front of the firing piezo-electric can receive ultrasonic waves (Fig. 2).

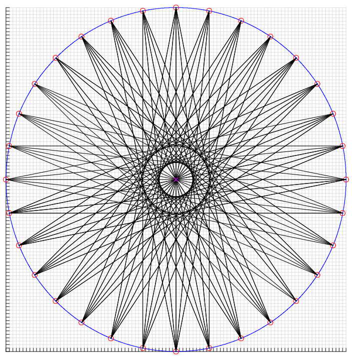

2-a

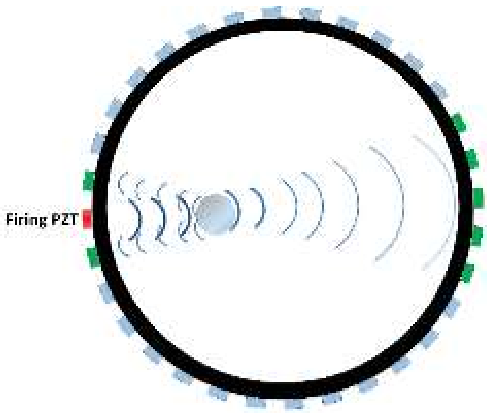

2-b

Fig. 2: Fan-shaped technique according to the far and near areas of the piezo-electric

Piezo-electrics, which are planted in front of the firing sensor, get the value of zero or one depending on the signal propagation time and the signal amplitude. Signal amplitude is calculated from the media attenuation coefficient. The value will be “one” if we receive the signal at a specified time with sufficient amplitude; otherwise, it will be “zero”.

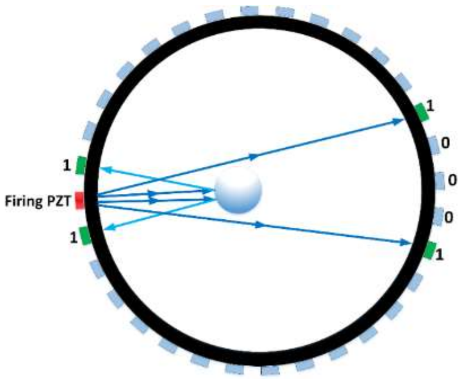

Fig. 3: Mode of receiving waves by piezo-electrics

Now if there is a bubble in this area, due to the position of the bubble inside the tube, some piezo-electrics in front of the transmitter cannot receive the signal (Fig. 3) because the direct path between the sender and receiver piezo-electric is closed and the signal is not received at the specified time and with an acceptable amplitude, which is related to the fact that ultrasound waves travel in a straight line [6]. Then in this case, the desired piezoelectric value is considered “zero” (Fig. 3). The aside piezo-electrics of the sender receive the reflection waves because the wave reflects from the gas/liquid interface. Depending on the reflection wave amplitude and its time of flight (TOF), the distance of the gas bubble from the sensors can be calculated.

A: Using the TOF technique

By using the TOF technique and according to Fig. 4, a vector can be found on which the bubble center is located with acceptable accuracy. The indicated vector is calculated as follows: vectors from the firing piezo-electric are plotted to the sensors that are assigned with “zero”, then their result, vector $\vec{T}$, is calculated for small bubble (Fig. 4-a), and big bubble (Fig. 4-b). The center of the gas bubble can be assumed on it with acceptable accuracy.

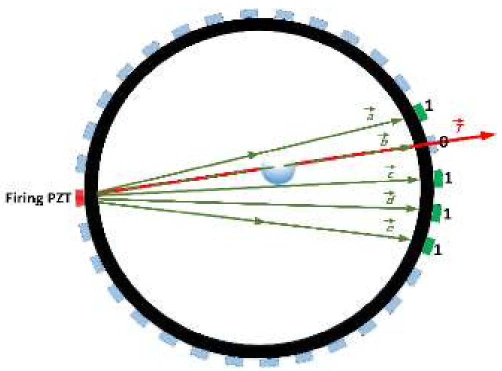

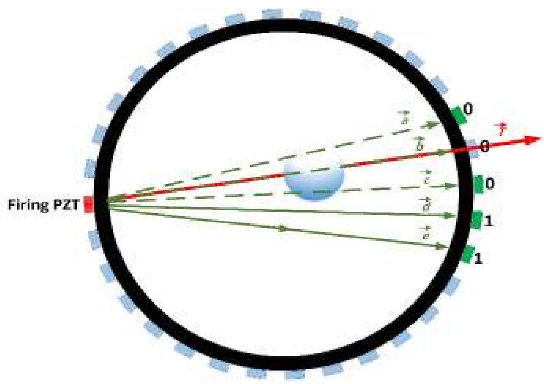

4-a: $\vec{T} = \vec{b}$ 4-b: $\vec{T} = \vec{a} + \vec{b} + \vec{c}$

Fig. 4: Calculating the result vector to locate the bubble place inside the tube

B: Using the Reflection mode

We used the reflected waves from the surface of the bubble to determine the circumference of the bubble. According to Fig. 5, if a bubble is located on the ultrasonic path, the waves reflect from the surface of the bubble depending on the position of the bubble and its size and due to a large difference in acoustic impedance between gas and liquid [22].

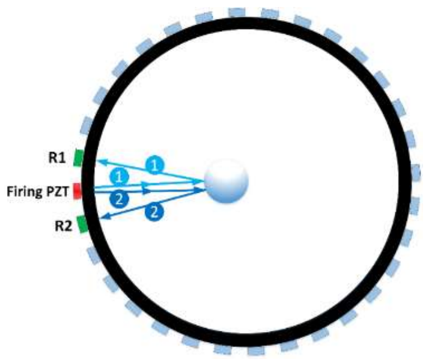

Fig. 5: Ultrasonic waves reflected from the surface of the bubble and receiving them by the side piezo-electrics

After hitting the ultrasound waves to the gas/liquid interface, waves propagate in all directions, and then they are received with sensors R1 and R2 from paths 1 and 2. Due to the propagation time of the ultrasonic waves between the firing and receiving sensors, we can calculate the incident point on the gas bubble. It should be noted in the wave propagation time calculation that the amplitude of the received signal is considered according to the amount of signal attenuation in the media. Also, the first high amplitude signal received by R1 and R2 is considered. According to Fig. 5, the bubble is directly opposite the firing piezo-electric, Thus, the return paths of the signals form an isosceles triangle. The point of the incident on the bubble is located on the perpendicular bisector of the firing and receiving piezo-electrics. This is a specific case that is mentioned in the previous articles [22]. But in Fig. 6, the other placement of the bubble inside of the pipe showed that it is different from the previous state. In Fig. 5, if the propagation time is divided by two, and according to the speed of the sound inside the media, we can determine the distance of the point of impact on the perpendicular bisector, and we will get the point of impact on the bubble exactly. This is the difference and capability of our technique that does not just check the specific mode for tomography.

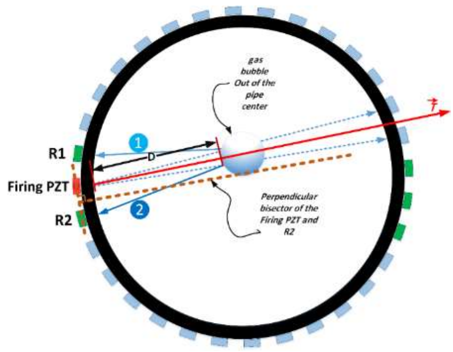

Fig. 6: Calculating the location of the bubble and its difference with the perpendicular bisector of the transmitter and receiver sensor

According to Fig. 6, it is pretty clear that by moving the bubble from the center of the tub to the other positions, the point of the waves and gas bubble collision is no longer on the equilateral perpendicular bisector of the firing and receiving piezo-electrics.

From section A and TOF technique, we have obtained the $\vec{\boldsymbol{T}}$ vector, which is the total vector of blind piezo-electrics. Blind sensors are sensors that do not receive a signal with sufficient amplitude at a given time. The proposed algorithm to reconstruct the cross-sectional image of the fluid flow is as follows: the propagation times of t1 and t2 were measured by R1 and R2 (Fig. 6). We obtained the traveled distances by the following simple equations:

$$l_1 = Vt_1 \quad (6)$$

$$l_2 = Vt_2 \quad (7)$$

where V is the ultrasound speed in the liquid and l1 and l2 are the distances that wave traveled at times t1 and t2, respectively. To obtain D, which is the distance between the firing piezo-electric and the bubble, the following simple equation can be used:

$$D = \frac{l_1 + l_2}{4} \quad (8)$$

We move on vector $\vec{\boldsymbol{T}}$ as much as D and determine the point where the waves hit the bubble. The simulation results show that the mentioned point is located on the gas bubble with high accuracy.

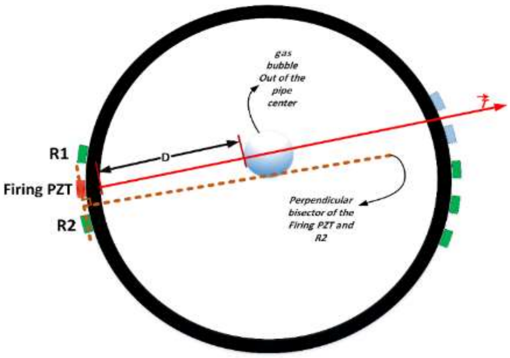

Fig. 7: Locating the hit point on the bubble with the proposed method

shaped method, points are obtained around the bubble. At the normal pressure and temperature, the gas bubble inside the liquid is spherical and each slice of it is circular [27]. We know that a circle can be drawn with three points, but to increase the algorithm's accuracy, more dots are obtained (Fig. 8). In this way, by changing the firing piezo-electric in the fan-

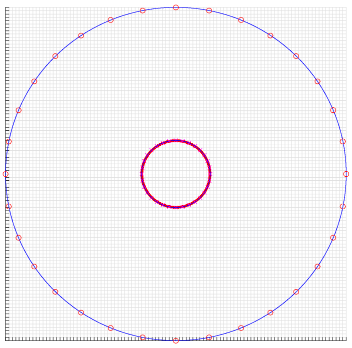

Fig. 8: Getting the dots around the bubble in the center of the tube

Now, by using a circle finder algorithm, an optimal circle can be passed over the points, which gives us a good approximation of the cross-sectional image of the gas bubble. There are many algorithms for doing this and we have used the V. Pratt method. This method is a robust and accurate circle fit. It works well even if data points are observed only within a small arc. This circle fit was proposed by V. Pratt and is called the V. Pratt method [28]

IV. Simulation Results

To measure the error of the proposed technique, we assume a bubble inside a tube with 32 piezo-electric sensors on it, and its cross-sectional image is depicted in Fig. (9).

We place the bubble inside the tube in different places, and the output of the algorithm for the cross-sectional image reconstruction is shown in Fig. 8. The reconstructed image of the gas bubble inside the tube is marked as a pallid circle which is not much different from the bubble marked by a bold circle. It is clear that as long as the calculated time for the reflected wave's propagation time is more accurate, the proposed method error is approaching zero. This propagation time is calculated by side piezo-electrics (R1 and R2). Figures 9-a and 9-b show that the reconstructed image for different positions of actual bubble, is placed on the bubble with reasonable accuracy.

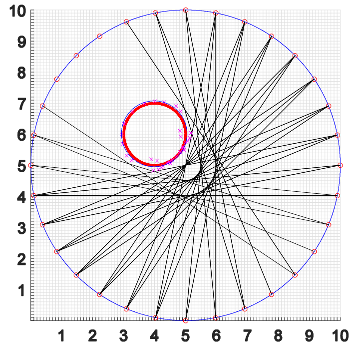

9-a

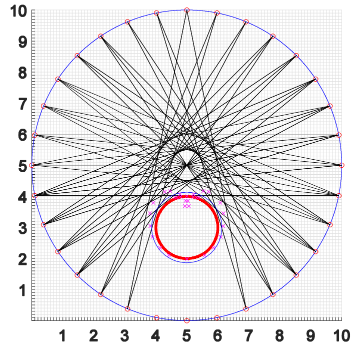

9-b

Fig. 9: Simulation results

The spatial imaging error (SIE) parameter is used to study the precision of simulations. This parameter is considered as including the total error of the set and is calculated in this way that the area of the reconstructed image is divided by the actual area of the bubble slice. We know that this value ought to be close to one [11]:

$$SIE = \frac{reconstructed\ \ surface\ of\ bubble\ slice}{real\ surface\ of\ bubble\ slice} \tag{9}$$

The relative error of the reconstructed images is presented by MATLAB simulation and it is much lower than the conventional methods. For a gas bubble that we have ultrasonic wave reflection time from its surface, the simulation results are depicted in Fig. 10, which is lower than 2%.

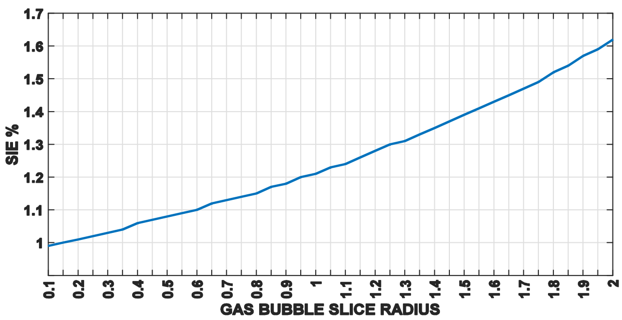

Fig. 10: The spatial imaging error (SIE) factor

V. Conclusion

In the proposed method, an ultrasonic transmission/reflection mode tomography is used for two-phase flow measurement. This measurement technique does not need artificial intelligence, complicated mathematical algorithms, and calibration systems. In addition, it does not need to know the flow pattern, so the measurement system is very stable. In this method, no shadow is formed for the gas bubble in image reconstruction. while in the filtered back projection algorithm (FBP) method with low sensor numbers or low radiation numbers, there is a shadow around the reconstructed bubble image. Table 1 presents some articles similar to the present paper. The simulation results show that the accuracy of the proposed method is acceptable. Given that the proposed method is simple and does not require sophisticated hardware or software, it ought to make system measurement faster. This algorithm does not need meshing to calculate the amount of fluid flow, and we can calculate that directly from the sensor's output data with a simple algebraic method. The relative error of the reconstructed images is presented by MATLAB simulation, which is lower than 2%. The accuracy of the proposed method depends on the number of the sensor and we can enhance the method's precision by increasing the number of sensors.

TABLE 1
COMPARISON OF SOME REFERENCES WITH THE PRESENTED ARTICLE

paper	Shadow in the reconstructed image	Reconstruction Algorithm	Fraunhofer zone	Tomography Method
[29]	has	Zernike polynomial	Not Considered	UTT
[22]	has	Filtered Back Projection	Considered	UTT/URT
[30]	has	Algebraic	Considered	UTT
This paper	Has not	Algebraic	Considered	UTT/URT

References

[1] Bidar, Bahareh, et al. "Soft Sensor Development for Monitoring ASTM-D86 Index: Effect of Feed Flow Rate Change." International Journal of Industrial Electronics Control and Optimization 4.2: 211-220, 2021.
[2] Ismail, Idris, et al. "Tomography for multi-phase flow measurement in the oil industry." Flow measurement and instrumentation 16.2-3: 145-155, 2005.
[3] Kirillov, K. M., et al. "An ultrasonic flowmeter for viscous liquids." Measurement Techniques 57.5: 533-536, 2014.
[4] Li, Nan, and Kun Xu. "Simulation study on ultrasonic tomography in bubbly gas/liquid two-phase flow." 2017

IEEE International Conference on Imaging Systems and Techniques (IST). IEEE, 2017.
[5] Qorbani, Omid, and Esmaeil Najafi Aghdam. "Two-Phase Flow Measuring with Ultrasonic Tomography." Archives of Acoustics: 459-465, 2020.
[6] Rymarczyk, Tomasz, et al. "Image reconstruction methods in radio and ultrasound tomography." 2018 International Interdisciplinary PhD Workshop (IIPhDW). IEEE, 2018.
[7] Safonov, A. V. "Experience with the use of ultrasonic flowmeters in systems for measuring the quantity and quality of petroleum." Measurement Techniques 57.4: 458-460, 2014.
[8] Wahab, Y. Abdul, et al. "Application of transmission-mode ultrasonic tomography to identify multiphase flow regime." International Conference on Electrical, Control and Computer Engineering 2011 (InECCE). IEEE, 2011.
[9] Duan, Xi, Panagiotis Koulountzios, and Manuchehr Soleimani. "Dual modality EIT-UTT for water dominate three-phase material imaging." IEEE Access 8: 14523-14530, 2020.
[10] Wang, Mi, ed. Industrial tomography: systems and applications. Elsevier, 2015.
[11] Xu, Lijun, et al. "Application of ultrasonic tomography to monitoring gas/liquid flow." Chemical Engineering Science 52.13: 2171-2183, 1997.
[12] Hanus, Robert, et al. "Evaluation of liquid-gas flow in pipeline using gamma-ray absorption technique and advanced signal processing." Metrology and Measurement Systems: 145-159, 2021.
[13] Cailly, William, et al. "Pipe two-phase flow non-invasive imaging using Ultrasound Computed Tomography: A two-dimensional numerical and experimental performance assessment." Flow Measurement and Instrumentation 74: 101784, 2020.
[14] Camacho, Jorge, et al. "Multimodal ultrasonic imaging for breast cancer detection." Archives of Acoustics 37: 253-260, 2012.
[15] Opieliński, Krzysztof, et al. "Ultrasound transmission tomography imaging of structure of breast elastography phantom compared to US, CT and MRI." Archives of Acoustics 38.3: 321-334, 2013.
[16] Rahiman, Mohd Hafiz Fazalul, Ruzairi Abdul Rahim, and Nor Muzakkir Nor Ayob. "The front-end hardware design issue in ultrasonic tomography." IEEE Sensors Journal 10.7: 1276-1281, 2010.
[17] Liang, Fachun, et al. "Gas–liquid two-phase flow pattern identification by ultrasonic echoes reflected from the inner wall of a pipe." Measurement Science and Technology 27.3: 035304, 2016.
[18] Goh, C. L., et al. "Ultrasonic tomography system for flow monitoring: A review." IEEE Sensors Journal 17.17: 5382-5390, 2017.
[19] Langener, Sascha, et al. "A real-time ultrasound process tomography system using a reflection-mode reconstruction technique." Flow Measurement and Instrumentation 53: 107-115, 2017.
[20] Rokhana, Rika, and Santi Anggraini. "Using of array of 8 ultrasonic transducers On accoustic tomography for image reconstruction." 2015 International Electronics Symposium (IES). IEEE, 2015.
[21] Staszewski, Wiktor, Tadeusz Gudra, and Krzysztof J. Opieliński. "The effect of dynamic beam deflection and focus shift on the acoustic field distribution inside the ultrasonic ring array." Archives of Acoustics: 625-636, 2019.
[22] Tan, Chao, et al. "An ultrasonic transmission/reflection tomography system for industrial multiphase flow imaging." IEEE Transactions on Industrial Electronics 66.12: 9539-9548, 2019.
[23] Dobrucki, A. B., and K. J. Opieliński. "Adaptation of image reconstruction algorithm for purposes of ultrasound transmission tomography (UTT)." Archives of Acoustics 25.4: 2000.
[24] Rupitsch, Stefan J. "Piezoelectric sensors and actuators." Simulation of Piezoelectric Sensor and Actuator Devices. In: Piezoelectric Sensors and Actuators. Topics in Mining, Metallurgy and Materials Engineering: 83-126, 2019.
[25] Taghvayi, Ebrahim, and Mohammad Reza Karafi. "A New Method to Detect and Track the Resonance Frequency of Piezoelectric Transducers in Ultrasonic Power Supplies." International Journal of Industrial Electronics Control and Optimization 4.4: 409-416, 2021.
[26] Ng, Alexander, and Justiaan Swanevelder. "Resolution in ultrasound imaging." Continuing Education in Anaesthesia Critical Care & Pain 11.5: 186-192, 2011.
[27] Bratland, Ove. "Pipe flow 2: multi-phase flow assurance." 41-59, 2010.
[28] Pratt V. Direct least-squares fitting of algebraic surfaces. ACM SIGGRAPH computer graphics. 1;21(4):145-52, Aug. 1987.
[29] Besic, Nikola, et al. "Zernike ultrasonic tomography for fluid velocity imaging based on pipeline intrusive time-of-flight measurements." IEEE transactions on ultrasonics, ferroelectrics, and frequency control 61.11: 1846-1855, 2014.
[30] Rahiman, MH Fazalul, R. Abdul Rahim, and Z. Zakaria. "Design and modelling of ultrasonic tomography for two-component high-acoustic impedance mixture." Sensors and Actuators A: Physical 147.2: 409-414, 2008.

Omid Qorbani was born in Malekan, East Azarbaijan, Iran. He received his B.S. degree in Electronics Engineering from the Amirkabir University of Technology, Tehran, Iran in 2004, and his M.S. degree from Electrical and Computer Faculty of Tabriz University, Tabriz, Iran in 2013. He is currently a Ph.D. candidate in Electronic Engineering at the Sahand University of Technology, Tabriz, Iran. He researches ultrasonic and ultrasonic flow-meters.

Esmaeil Najafiaghdam achieved his Ph.D. on Delta Sigma ADC at Paris-Sud in 2006. He is now a Professor of Electronics Eng. at the Sahand University of Technology. His research interests include Delta Sigma converters, RF, and ultrasonic.

IECO
This page intentionally left blank.